Synthesis and characterization of Fe_3O_4@Cs@Ag nanocomposite and its use in the production of magnetic and antibacterial nanofibrous membranes

Aylin YILDIZ[1], Derman VATANSEVER BAYRAMOL[2,*], Rıza ATAV[1], A. Özgür AĞIRGAN[1], Mine AYDIN KURÇ[3], Uğur ERGÜNAY[1], Carl MAYER[4], Ravi L. HADIMANI[5, 6]

***corresponding author: derman.bayramol@alanya.edu.tr**

[1]Faculty of Engineering, Department of Textile Enginnering, Tekirdağ Namık Kemal University, Çorlu-Tekirdağ, Turkey

[2]Department of Metallurgical and Materials Engineering, Alanya Alaaddin Keykubat University, Alanya-Antalya, Turkey

[3]School of Medicine, Department of Microbiology, Tekirdağ Namık Kemal University, Tekirdağ, Turkey

[4]Nano Characterization Center, Virginia Commonwealth University, Richmond VA 23284, USA

[5]Department of Mechanical and Nuclear Engineering, Virginia Commonwealth University, Richmond VA 23284, USA

[6]Department of Biomedical Engineering, Virginia Commonwealth University, Richmond VA 23284, USA

Abstract

Electrospinning is a pomising technique to produce polymeric as well as metal oxide nanofibers in diverse domains. In this work, different weight ratios (5%, 7.5% and 10%) of Fe_3O_4@Cs@Ag magnetic nanoparticles were added in PVP (polyvinylpyrrolidone) polymer and fabricated via electrospinning method to produce magnetic nanofibers (MNFs). Structural, magnetic, morphological, spectroscopic and thermal properties of produced nanofibers were characterized. Furtheremore, antibacterial effects of Fe_3O_4@Cs@Ag nanofibrous membrane

was investigated. Obtained SEM images showed that produced nanofibers were uniform and defect free. Moreover, crystallinity and magnetic moment of fibers was tested by using X-ray diffraction and a vibrating sample magnetometer. The results showed that produced nanofibrous membranes exhibited good antibacterial activity versus *Staphylococcus aureus, Bacillus subtilis, Enterococcus faecalis, Escherichia coli, Proteus mirabilis and Pseudomonas aeruginosa.*

Keywords: Fe_3O_4@Cs@Ag, nanofiber, magnetic property, antibacterial activity

1. Introduction

Electrospinning is a technique that allows the production of very fine diameters through the electrostatic force created between the two electrodes. This fiber production technique has a potential to be used in diverse fields therefore, lately, a significant number of studies have been concentrated on nanoscale fiber production [1]. To produce nanofiber structures via electrostatic force, both natural and synthetic polymers can be used as raw materials polymer solution [2]. The advantages of using electrospinning technique are porosity, ductility, high specific surface area, fine diameter of fibers ranges from several nanometers to several microns, controllability and design of the fiber formation [3]. Therefore, it can be considered as a versatile technique for nano-scale fiber composites and porous structures. Electrospun nanofiber structures have a wide range of applications including but limited to filtration, material reinforcement, energy storage, wound dressings and so on. [4-6].

The interest in developing new nanomaterials has aroused recently due to its wide range of potential applications in multiple fields [7-10]. Magnetic and optical properties of magnetic nanomaterials make them good candidates for different research areas and multidiciplinar studies. A significant number of magnetic nanoparticles are synthesized however, Fe_3O_4 is the

most widely studied one due to its properties such as optical, electrical, spin dependent transport, super-paramagentism and low toxicity [11, 12]. Furtheremore, Fe_3O_4 can be considered as environmental friendly and it is low in price.

Unique properties of Fe_3O_4 attracted great attention in various applications, such as magnetic recording media [13], drug delivery agents [14] and adsorbents [15, 16]. Fe_3O_4 nanoparticles are good candidates for magnetic attenuation sources in electromagnetic shielding composites due to their excellent magnetic and dielectric properties [17]. Biotechnology/biomedicine, medical diagnosis, electrochemical and bioeletrochemical sensing, environmental remediation, catalysis, electrodes for supercapacitors and lithium ion batteries, data storage, magnetic fluids recording, photo catalysis, microwave absorption, material sciences, magnetic resonance imaging are some of the potential applications for Fe_3O_4 and its nanocomposites [18-25]. Lately studies in the literature have focused on the use of magnetic nanoparticles as carriers of drug or gene delivery and as contrast agents for magnetic resonance imaging biomolecules separation [26].

Chitosan is an aminopolysaccharide biopolymer derivated derived by N-deacetylation of chitin, whose structure may be regarded as cellulose, but chitin has acetamide groups ($-NHCOCH_3$) instead of the hydroxyl [-OH] at the C2-portion [27]. It is a linear polycation with high charge density, reactive hydroxyl and amino groups as well as extensive hydrogen bonding. Its biocompatibility, physical stability and processability make chitosan important for a number of applications [28]. Chitin is characterized as white, non-elastic, hard, nitrogenous polysaccharides that have been estimated to be synthesized in approximately one billion tons annually [29, 30]. Chitosan is derivated from chitin, which can be found in nature, as the structural component of crabs, shrimps, lobsters, and insects, in algae, and some fungal cell walls [31, 32]. Chitosan is composed of β (1→4)-linked 2-acetamido-2-deoxy-β-D-glucose (N-

acetylglucosamine). Chitosan can also be obtained from dimorphic fungi, such as *Mucor rouxii*, by the action of the deacetylase enzyme on chitin [33-35]. Due to its high biodegradability, nontoxicity and antimicrobial properties, a significant number of applications of chitosan is to use it as an antimicrobial agent either alone or blended with other natural polymers [36]. Important properties of chitosan and its oligosaccharides include: antifungal and antibacterial [37, 38]; anti-inflammatory [39]; antitumour [40]; neuroprotective [41].

Textile fabrics have a potential to be used in many applications due to their versatility and ease to combine with composite materials [42]. Production of technical and functional textiles can be considered as important milestones in textile industry. One of the most desired functionality in textiles is being antibacterial for not only in medical applications but also in daily life. Therefore, production of antibacterial textiles has increased for a number of application areas, including but not limited to hygienic and medical applications. Conductive textiles are very promising to be used for electromagnetic shielding issues in the field of industry, military and civil wearable technologies as well as medicine, telecommunication [43]. There are a number of electromagnetic shielding applications of nonwoven and nonwoven coated fabrics with conductive fibers due to their light-weight, flexibility, versatility and grate blending options [44]. One of the material which is desirable for industrial applications, where good conductivity, chemical stability, and catalytic and antibacterial activity required, is collodial silver [45]. Silver has been a potential material for medical applications since ancient times due to antibacterial, antifungal and antivirus effects of silver ions. [46-48]. A complex compound of silver was previously synthesized and used as an antibacterial agent in finishing process of a cotton fabric [49]. Using silver ions in a complex compound offers some advantages, such as not getting into the skin when contacted that makes it possible to be used as a new antibacterial agent in textiles [49, 50].

In a master thesis fulfilled by Demir, Fe_3O_4@HumicAcid@Ag magnetic nanocomposites were synthesized via a simple reflux method. Produced nanocomposites were added in a polymer solution and drawn via an electrical force to form magnetic nanofibers. The analyzes conducted in the thesis proved that produced nanofibers were in a size range between 200 nm and 400 nm, and they had both antibacterial and magnetic properties [50]. In another study, inclusion complexes of Fe_3O_4@HumicAcid@Ag and β-CD were prepared via kneading technique to gain water solubility [51].

The aim of this study was to produce nanofibers including Fe_3O_4, chitosan (Cs) and Ag in the structure to obtain both magnetic and antibacterial properties. The antibacterial effect of chitosan has been known for a long time. Therefore, it was predicted to have an increase in the antibacterial effect in the composite nanofibers by adding chitosan into the composite structure. For this purpose, first of all, a nanocomposite material consisting of Fe_3O_4, chitosan (Cs) and Ag was synthesized and characterized. Then, synthesized Fe_3O_4@Cs@Ag nanocomposites were added into polyvinylpyrrolidone (PVP) polymer solution. Magnetic nanoparticle containing polymer solution was fed to a single capillary electrospinning unit to produce nanofibers. Produced Fe_3O_4@Cs@Ag doped PVP nanofibers were then tested to investigate their antibacterial activity and also magnetic property.

2. Experimental

2.1. Chemicals and instrumentations

$FeCl_3.6H_2O$, $FeCl_2.4H_2O$, $AgNO_3$, $NaBH_4$, NH_3 and DMSO (Dimethyl sulfoxide) were obtained from Merck (Darmstadt, Germany). High purity chitosan ($C_6H_{12}NO_4$, Mv 50,000-190,000), polyvinylpyrrolidone $(C_6H_9NO)_X$, M_W=1.300.000), N,N-dimethylformamide (DMF) and ethanol were purchased from Aldrich and used without further purification. DMEM

(Dulbecco's modified Eagle's high glucose medium) and Fetal bovine serum (FBS) were obtained from Capricorn (Capricorn Scientific, Ebsdorfergrund, Germany), while MTT [3-(4 5-dimethylthiazol-2-yl)-2 5-diphenyltetrazolium bromide] was purchased from Serva (Heidelberg, Germany). Nutrient broth and Mueller Hinton (MH) agar were obtained from Diffco (Difco, Detroit, USA).

Produced nanocomposites were analysed via a BRUKER VERTEX 70 ATR model Fourier alternating infrared spectrometer (FT-IR-ATR) in ytansmission mode over the range of 400-4000 cm^{-1}. For obtaining information on crystalline structure and surface morphology of produced materials, PANalytical Empyrean brand X-ray diffraction (XRD) equipment and Quanta FEG 250 model Scanning Electron Microscope (SEM) (FEI, Netherland) were used, respectively.

Magnetic measurements of samples were carried out in Quantum Design's Dynacool superconducting magnetometer that has a field range of -9 T to +9T and a temperature range of 1.9K to 1000K. A Perkin Elmer Instruments brand DSC 4000 model thermogravimetric analyser was used to determine the thermal stability of the materials. For the thermogravimetric analyse, 6 mg of each sample was heated with a heating rate of 10°C/min under nitrogen atmosphere and the results were recorded. Production of nanowebs were carried out via Inovensa, Inc. brand single-capillary electrospinning device, which allows both horizontal and vertical production.

2.2. Preparation of Fe_3O_4@Cs@Ag nanocomposite

A study in the literature was followed for the preparation of Fe_3O_4@Cs@Ag nanocomposite [48]. $FeCl_3.2H_2O$ and $FeCl_2.4H_2O$ salts with a molar ratio of 2:1, and 2 g of chitosan ($C_6H_{12}NO_4$, Mv 600,000-800,000) were placed in a three-neck flask to obtain Fe_3O_4@Cs. After a homogeneous solution was obtained by stirring at 40°C for 15 min, the pH of the solution was

increased to pH ~11-12 by adding NH_3 drop wise. Then obtained black material was put into a reflux, and continuously stirred at 80°C for 2 h in the presence of argon gas. Magnetic decantation method was used to seperate Fe_3O_4@Cs from the aqueous solution. Seperated Fe_3O_4@Cs was then washed with distilled water several times and dried in the oven at 80°C for 4 h. Obtained Fe_3O_4@Cs was sonicated in 100 mL of deionized water for an hour. After addition of 0.2 mmol/L of $AgNO_3$ solution in to the mixture, a further ultrasonication was applied for 2 h followed by rapid edition of 0.6 g of $NaBH_4$. The whole mixture was vigorously stirred for 2 h to allow the reaction. The separation of final nanocomposite (Fe_3O_4@Cs@Ag) was done magnetically. To eliminate any impurities, obtained Fe_3O_4@Cs@Ag was washed with deionized water for several times.

2.3. Production of nanofibrous membranes containing Fe_3O_4@Cs@Ag

Polymer solution, consisting of PVP and absolute ethanol with a ratio of 18% w/v was prepared while three different weight ratios (5%, 7.5% and 10%) of Fe_3O_4@Cs@Ag were homogenously dispersed in DMF (10 mL). These two mixtures were put together and stirred vigorously at 50°C for 6 h to prepare the electrospinning solution. Viscosity and conductivity values of the prepared solutions were as given in Table 1.

Table 1. Viscosity and conductivity values of prepared PVP solutions containing different ratios of Fe_3O_4@Cs@Ag

Fe_3O_4@Cs@Ag (%)	5	7.5	10
Viscosity (cP)	893.8	773.8	707.8
Conductivity (µS/cm)	35.2	37.1	38.3
Temperature (°C)	23.6	23.6	23.6

Prepared solution was used in electrospinning device via a 10 mL syringe and a syringe pump. The inner diameter of the capillary was 0.7 mm. Pretrials were done to determine the optimum electrospinnig parameters for this particular study. The optimum parameters were found to be 0,5 mLh^{-1} feeding rate, 17.5 kV high voltage, and 15 cm distance between the capillary tip and the collector.

2.4. Determination of antibacterial activity

In our study, antibacterial activity of Fe_3O_4@Cs@Ag nanofiber was determined by using disk diffusion method. *Staphylococcus aureus* (ATCC 29213), *Bacillus subtilis* (NRRL NRS-744), *Enterococcus faecalis* (ATCC 29212), *Escherichia coli* (ATCC 25922), *Proteus mirabilis* (ATCC 12453) and *Pseudomonas aeruginosa* (ATCC 27853) were used as test microorganisms in this study. Bacteria strains were inoculated to nutrient agar and were then activated by incubating at 37°C for 16-24 hours. After incubation, bacteria density was adjusted to 0.5 MacFarland at Mueller Hinton Broth for all microorganisms and then, Mueller Hinton agar were inoculated with a density-adjusted bacterial suspension. Fe_3O_4@Cs@Ag composite in three different concentrations (I: 5%, II: 7.5%, III: 10%) were tested for antibacterial activity. In addition, DMF solution were used as a negative control in the synthesis of the nanofibers and gentamicin disk were also used as a positive control. 5 µl of the prepared test samples (I, II, III and DMF) were impregnated onto sterilized discs prepared by cutting 5 mm pieces from Whatman Filter paper. Prepared samples were placed on plates that were then incubated at a temperature of 37±2°C for 24 hours. Inhibition zone diameters (milimeter) were measured at the end of incubation. Each test was performed three times.

3. Results and Discussion

3.1. Characterization of magnetic nanofibers containing Fe_3O_4@Cs@Ag

The Fe_3O_4@Cs@Ag nanocomposites obtained as a result of synthesis were separated from the medium by a magnet. Therefore, the obtained product definitely contained Fe_3O_4. For determination whether it also contains Cs and Ag, in other words whether the nanocomposite formation occurred or not, FTIR, XRD, TGA, SEM-EDX, and VSM analysis were performed and the results were presented below.

FTIR spectra of the pure chitosan, Fe_3O_4@Cs and Fe_3O_4@Cs@Ag given in Figue 1 confirm that the syntheses of nanoparticles were successful. The peak observed at 3364 cm^{-1} on transmission spectra of chitosan was related to the amino (-NH_2) and hydroxyl (-OH) groups. The band at 1649 cm^{-1} was attributed to C=O stretching vibration of amide groups while the band at 1590 cm^{-1} represented to the bending vibration of -NH_2 groups. The C-O stretching vibration of C-OH was observed at 1059 cm^{-1} in the spectrum. The peaks observed in the transmission spectrum of chitosan were at 3364, 1649, 1590 and 1059 cm^{-1}. These peaks shifted to 3358, 1632, 1560 and 1018 cm^{-1}, respectively, in the spectrum of Fe_3O_4@Cs nanocomposites. On the other hand, when the spectrum of Fe_3O_4@Cs@Ag MNFs was analyzed, it can be seen that the peaks shifted to 3340, 1627, 1556, 1041 cm^{-1}. Therefore, obtained results clearly indicated the involvement in complexation of amino and hydroxyl groups of chitosan with Fe^{3+}. Moreover, in the spectrum of Fe_3O_4@Cs, the strong peak observed at 559 cm^{-1} was related to the Fe-O bond vibration of Fe_3O_4, which were observed at 546 cm^{-1} for Fe_3O_4@Cs@Ag [52].

Fe_3O_4@Cs@Ag MNFs containing 5%, 7.5% and 10% of Fe_3O_4@Cs@Ag were also studied under FT-IR for their surface chemisty. The stretching vibrations of Fe-O bond were seen in Figure 1 as a broad peak centered at ~550 cm^{-1} when transmission spectra of Fe_3O_4@Cs@Ag

and magnetic nanofibers were studied. The peek seen at ~1650 cm^{-1} of the spectrum of Fe_3O_4@Cs@Ag MNFs was attributed to attributed to C=O stretching vibration of amide groups while the stretching bands at ~1280, ~2900 cm^{-1} detected in the spectrum were related to -CH_2, -CH_3 species, respectively [53]. Therefore, it is possible to claim that obtained nanofibers contain magnetic particles of Fe_3O_4@Cs@Ag with regard to the transmission spectrums obtained from FT-IR. The crystal structures and phase investigation of Fe_3O_4@Cs@Ag MNFs (5%, 7.5% and 10%) were performed, and the patterns obtained from XRD are shown in Figure 2b. The existence of both Fe_3O_4 ((220), (311)) (JCPDSNo.75-0033)) and Ag (111) (JCPDSNo.87-0720) was confirmed in XRD patterns of MNFs containing 7.5% and 10% of Fe_3O_4@Cs@Ag [54, 55]. However, these peaks were not observed in the XRD pattern of MNFs containing 5% Fe_3O_4@Cs@Ag.

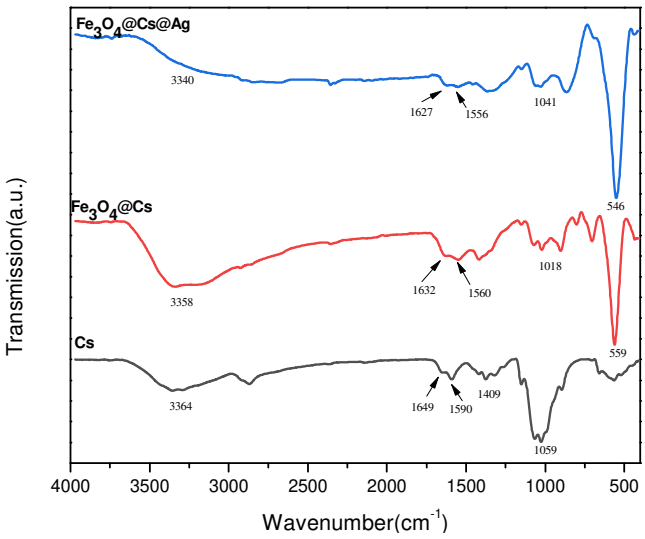

Figure 1: FT-IR specta of Fe_3O_4@Cs@Ag nanocomposite

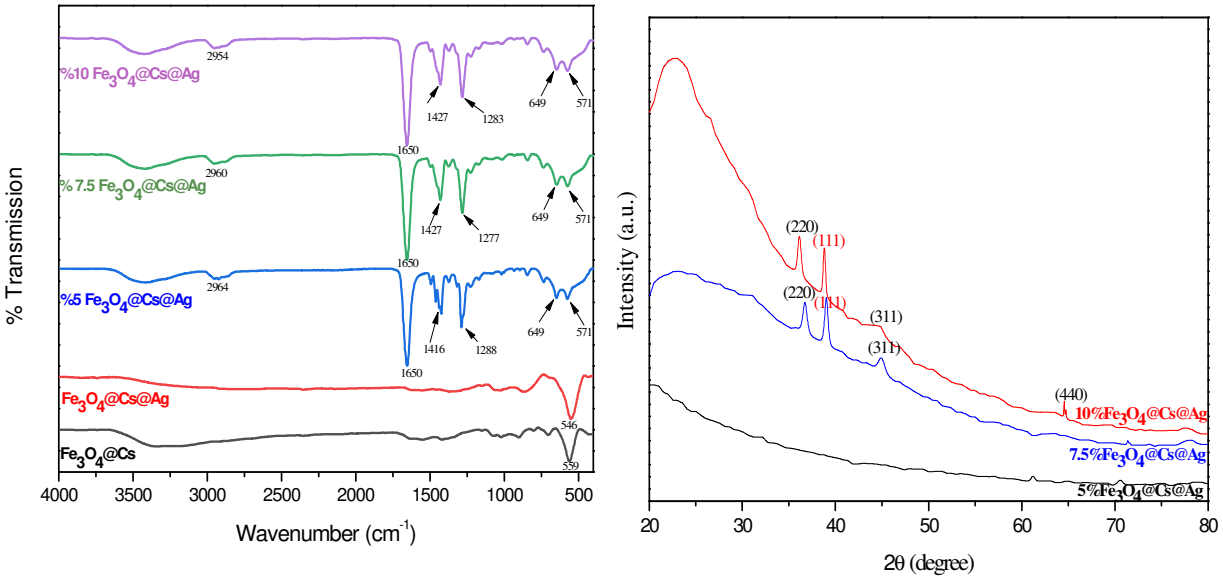

(a) **(b)**

Figure 2. (a) FT-IR spectra of Fe_3O_4@Cs nanocomposite, Fe_3O_4@Cs@Ag magnetic nanocomposite and Fe_3O_4@Cs@Ag MNFs (5%, 7.5% and 10%); **(b)** XRD patterns of Fe_3O_4@Cs@Ag magnetic nanofibers (5%, 7.5% and 10 %)

TGA thermograms of the Fe_3O_4@Cs nanocomposite, Fe_3O_4@Cs@Ag magnetic nanocomposite and Fe_3O_4@Cs@Ag MNFs (5%, 7.5% and 10%) are given in Figure 3. For Fe_3O_4@Cs and Fe_3O_4@Cs@Ag nanocomposites, weight loss occurred between 250°C and 500°C are connected with the decomposition of chitosan. As Fe_3O_4@Cs@Ag nanocomposite contain lower chitosan amount in weight (%), weight loss was not as sharp as Fe_3O_4@Cs. On the other hand, the evident peak observed in TGA thermograms of the Fe_3O_4@Cs@Ag MNFs between 450 and 500°C are related to the decaying of chitosan and ignition of PVP.

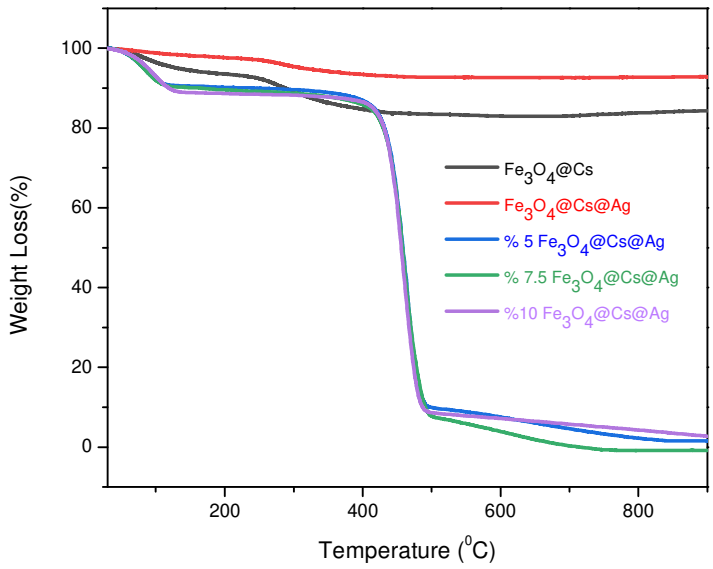

Figure 3. TGA thermograms of Fe_3O_4@Cs nanocomposite, Fe_3O_4@Cs@Ag magnetic nanocomposite and Fe_3O_4@Cs@Ag MNFs (5%, 7.5% and 10%)

The surface morphology of Fe_3O_4@Cs@Ag/PVP MNF nanowebs containing 5%, 7.5% and 10% Fe_3O_4@Cs@Ag can be seen from the SEM images given in Figure 4. It can be said that successful and bead free magnetic nanofiber production was confirmed by the SEM images. It should be noted that the distribution of fiber diameter was between 200 nm and 500 nm.

The chemical composition of Fe_3O_4@Cs@Ag MNFs were determined with a quantitative elemental analysis from EDX measurements. Obtained EDX spectra of Fe_3O_4@Cs@Ag MNFs are shown in Figure 5. An increase in the amount of Ag and Fe was detected in EDX graphs due to the increase in Fe_3O_4@Cs@Ag in electrospinning solution. Figure 6 clearly shows the increase in the amount of Ag and Fe, with an increase in the amount of magnetic nanocomposites in the nanofiber structure. This confirms the successful electrospinning process and magnetic nanofiber production.

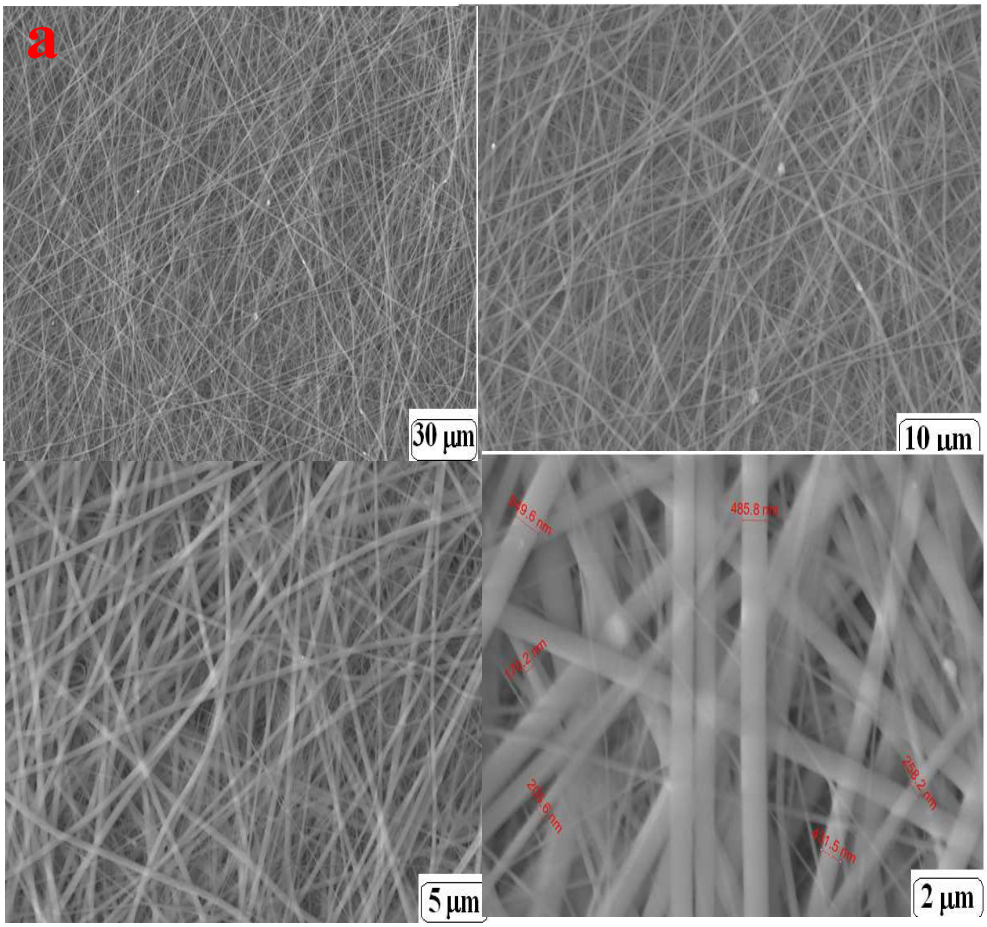
a
30 µm
10 µm
5 µm
2 µm
485.8 nm

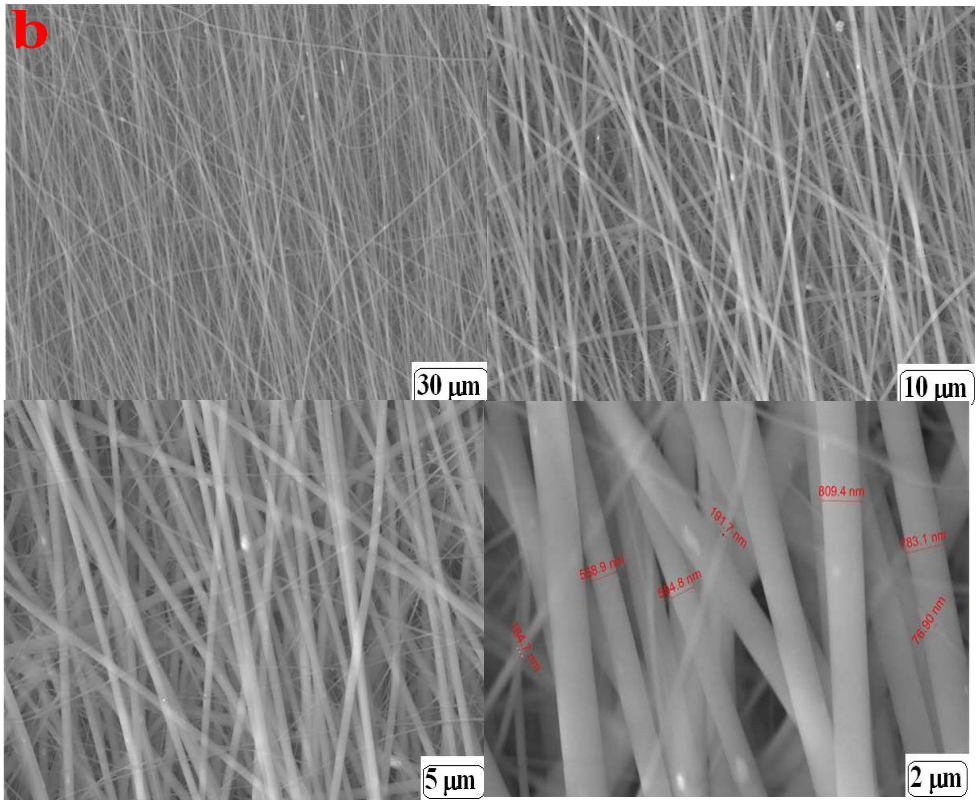
b
30 µm
10 µm
5 µm
809.4 nm
191.7 nm
183.1 nm
559.9 nm
584.8 nm
764.90 nm
2 µm

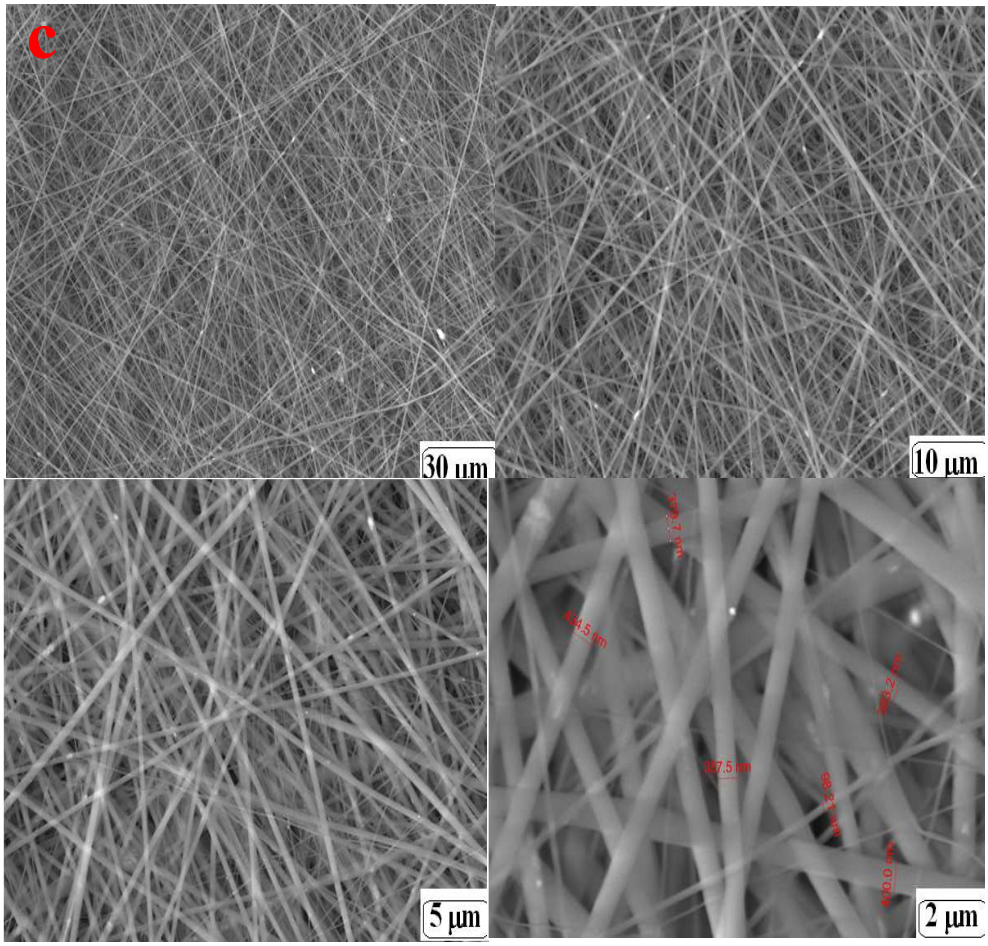

Figure 4. SEM images of magnetic nanofibers containing **(a)** 5%; **(b)** 7.5% and **(c)** 10% Fe_3O_4@Cs@Ag in the fiber structure

.

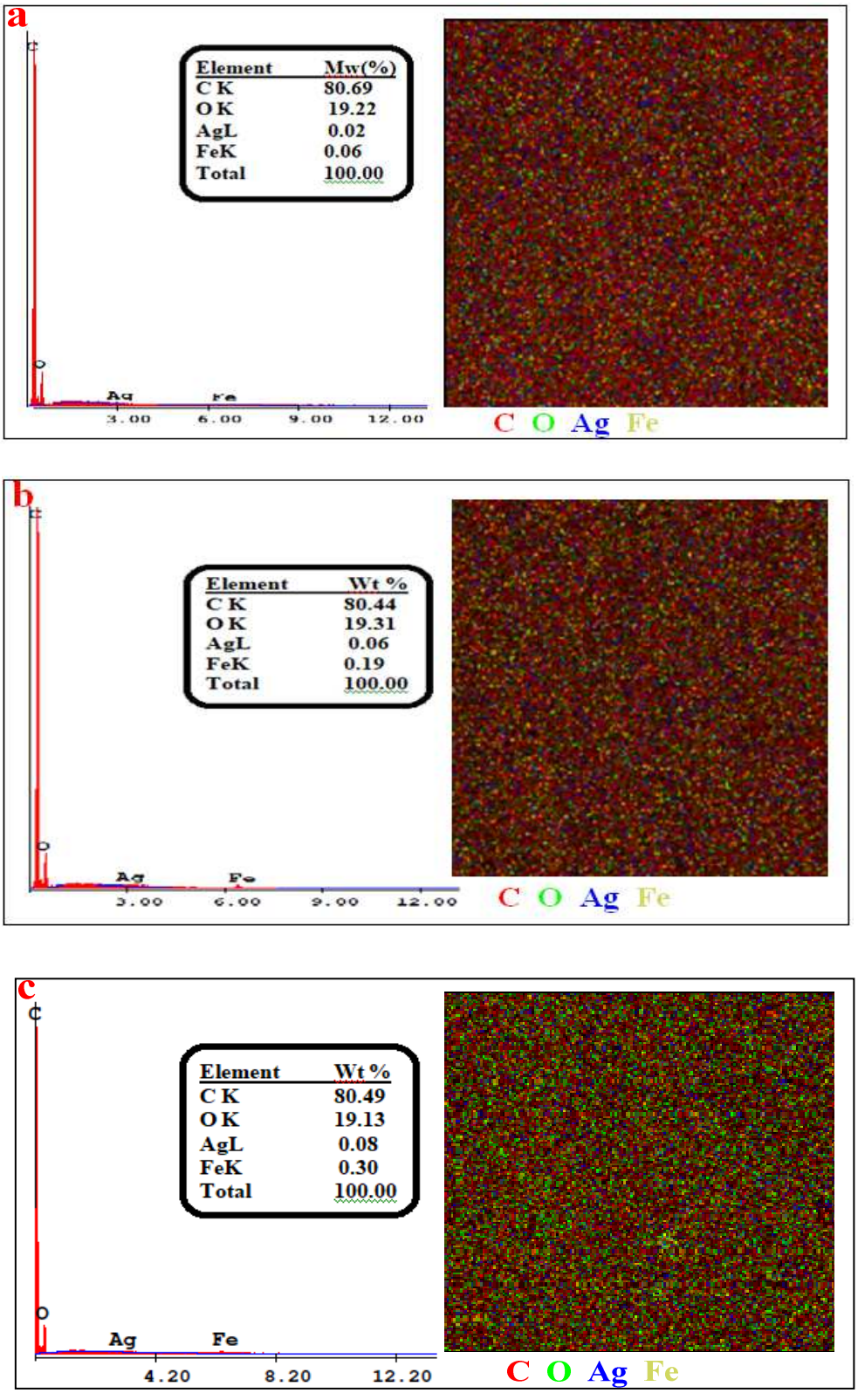

Figure 5. EDX spectra of magnetic nanofibers containing (a) 5%; (b) 7.5% and (c) 10% of Fe_3O_4@Cs@Ag in the fiber structure

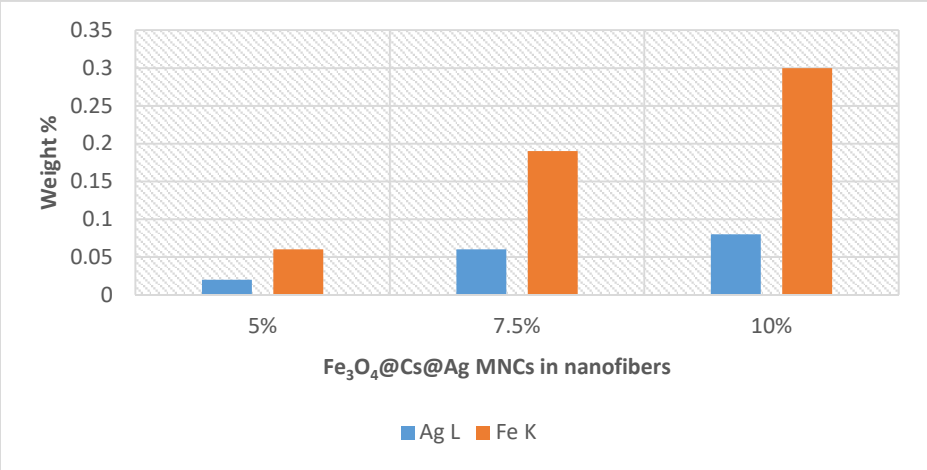

Figure 6. Amount of Ag and Fe in magnetic nanofibers containing 5%, 7.5% and 10% of Fe_3O_4@Cs@Ag in the fiber structure

Magnetic measurements of samples were also carried out. Figure 7 (a)-(c) show magnetization as a function of magnetic field for 5%, 7.5% and 10% Fe_3O_4@Cs@Ag measured at a temperature of 300 K. The inset figures in Figure 7 a, b, c show the magnified portion of the hysteresis graphs highlighting small coercivity. 5%, 7.5% and 10% Fe_3O_4@Cs@Ag have a coercivities of 20 Oe, 20 Oe and 25 Oe respectively. Figure 7 (d) shows hysteresis graphs of all 3 samples between magnetic field range of +3T to -3T (+30 kOe to -30 kOe) at an interval of 100 Oe. It can be noted that hysteresis graphs do not saturate even at an applied magnetic field of 30 kOe. This is because of the paramagnetic nature of PVP in the samples. The paramagnetic fraction of the sample contributed by PVP was deducted by first calculating the slope of the magnetic curve above 1 T (10 kOe) magnetic field and subtracting it in the original hysteresis graphs. The saturation field of 1 T (10 kOe) was chosen based on the prior literature on Fe_3O_4 [17, 44, 56, 57]. Figure 7 (e) shows hysteresis graphs of 5%, 7.5% and 10% Fe_3O_4@Cs@Ag after removing the paramagnetic contribution from the original hysteresis graphs. The coercivity and the remanence magnetization of the hysteresis graph didn't change significantly after the removal of paramagnetic contribution of PVP.

Saturation magnetization of high purity Fe_3O_4 nanoparticles range from 80 emu/g to 100 emu/g based on the method of preparation [17, 44, 56-58]. The saturation magnetic field of pure Fe_3O_4 nanoparticles is reported to be below 10kOe [17, 56]. However, the saturation magnetization of composite materials that have magnetic nanoparticles will be significantly smaller due to contribution of mass of non-magnetic constituent of the composite material.

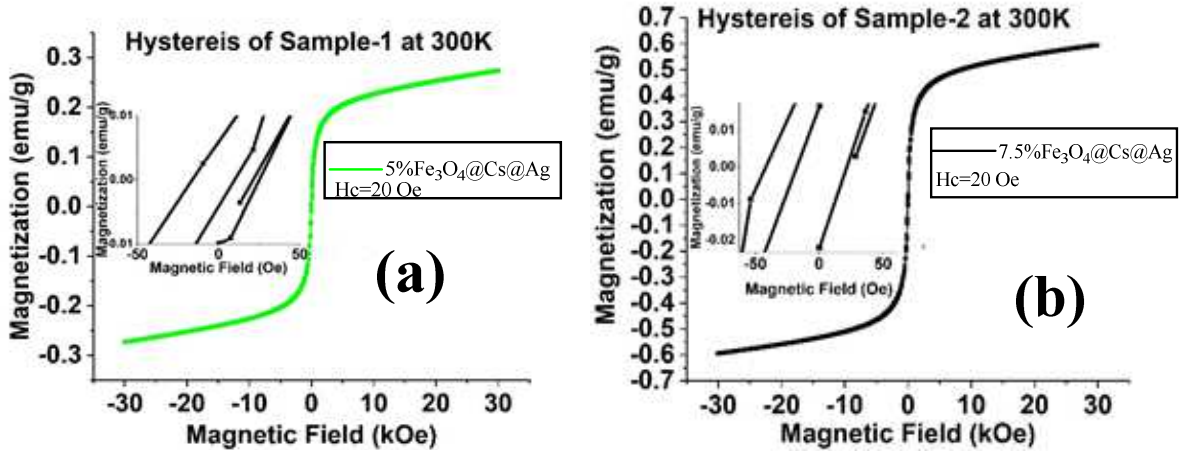

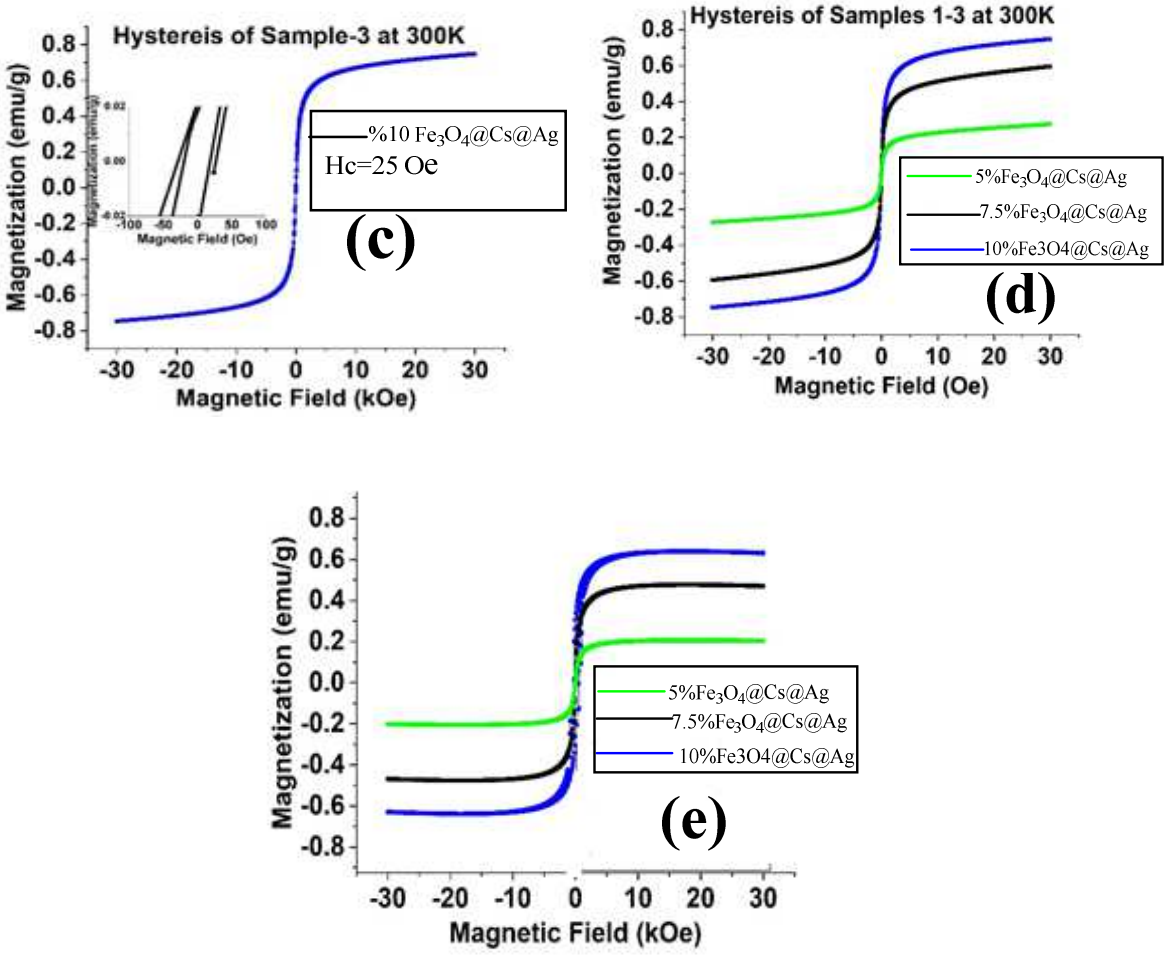

Figure 7. Magnetization as a function of magnetic field measurements at 300 K on (a) sample 1 (b) sample 2 (c) sample 3. Inset of (a), (b) and (c) graphsshow coercivity of 20 Oe, 20 Oe and 25 Oe respectively. (d) shows combined hysteresis graphs between 3T (30 kOe) and -3T (30 kOe) and (e) shows hysteresis graph after removal of paramagnetic part of PVP.

It can be attributed that the reduced saturation magnetization detected in the samples could be caused by following circumstances; surface spins canting, which was resulted by competing antiferromagnetic interactions [54], randomly dispersed small particles exhibiting high magneto-crystalline anisotropy caused unsaturation effect [55], spin glass characteristics [56], magnetic inactive layer formation [57] and the disordering cations distribution [17] on the surface of nanoparticles.

Table 2 shows saturation magnetization, remanence magnetization in emu/g, ratio of remanence and saturation magnetization and coercive fields for 5%, 7.5% and 10% Fe_3O_4@Cs@Ag at room temperature. These values are derived from Figure 7. All the three samples show very low coercive fields and low remanence magnetization. The ratio of remanence and saturation magnetization is also significantly below 0.5, indicating that the magnetic nanoparticles are soft ferromagnetic and have uniaxial anisotropy [59].

Table 2. Magnetic properties of 5%, 7.5% and 10% Fe_3O_4@Cs@Ag doped PVP nanofibers

Rate (wt %)	**M_s (emu/g)**	**M_r (emu/g)**	**M_r/M_s**	**H_c (Oe)**
5% Fe_3O_4@Cs@Ag	0.47	0.009	0.019	20
7.5% Fe_3O_4@Cs@Ag	0.20	0.02	0.1	20
10% Fe_3O_4@Cs@Ag	0.63	0.03	0.048	25

3.2. Determination of antibacterial activity

The antibacterial activities by disk diffusion method of inhibiton zones of Fe_3O_4@Cs@Ag magnetic nanofibers were given in Table 3 and Figure 8. As it could be seen from Table 3 the antibacterial activity increased depending on concentration levels.

Table 3. Inhibiton zones of Fe_3O_4@Cs@Ag MNFs in mm

	S. aureus **ATCC 29213**	***B. subtilis*** **NRRL NRS-744**	***E. faecalis*** **ATCC 29212**	***E. coli*** **ATCC 25922**	***P. mirabilis*** **ATCC 12453**	***P. aeruginosa*** **ATCC 27853**
I	ND	ND	8.33±0.57	7.33±0.57	7.0±1.0	ND
II	6.66±0.57	ND	8.66±0.57	7.66±0.57	7.33±0.57	6.33±0.57

III	8.0±1.0	6.33±057	8.66±0.57	9.0±1.0	8.33±0.57	7.66±0.57
DMF	ND	ND	ND	ND	ND	ND

Values are mean of triplicate readings (mean ± S.D). ND= Not detected

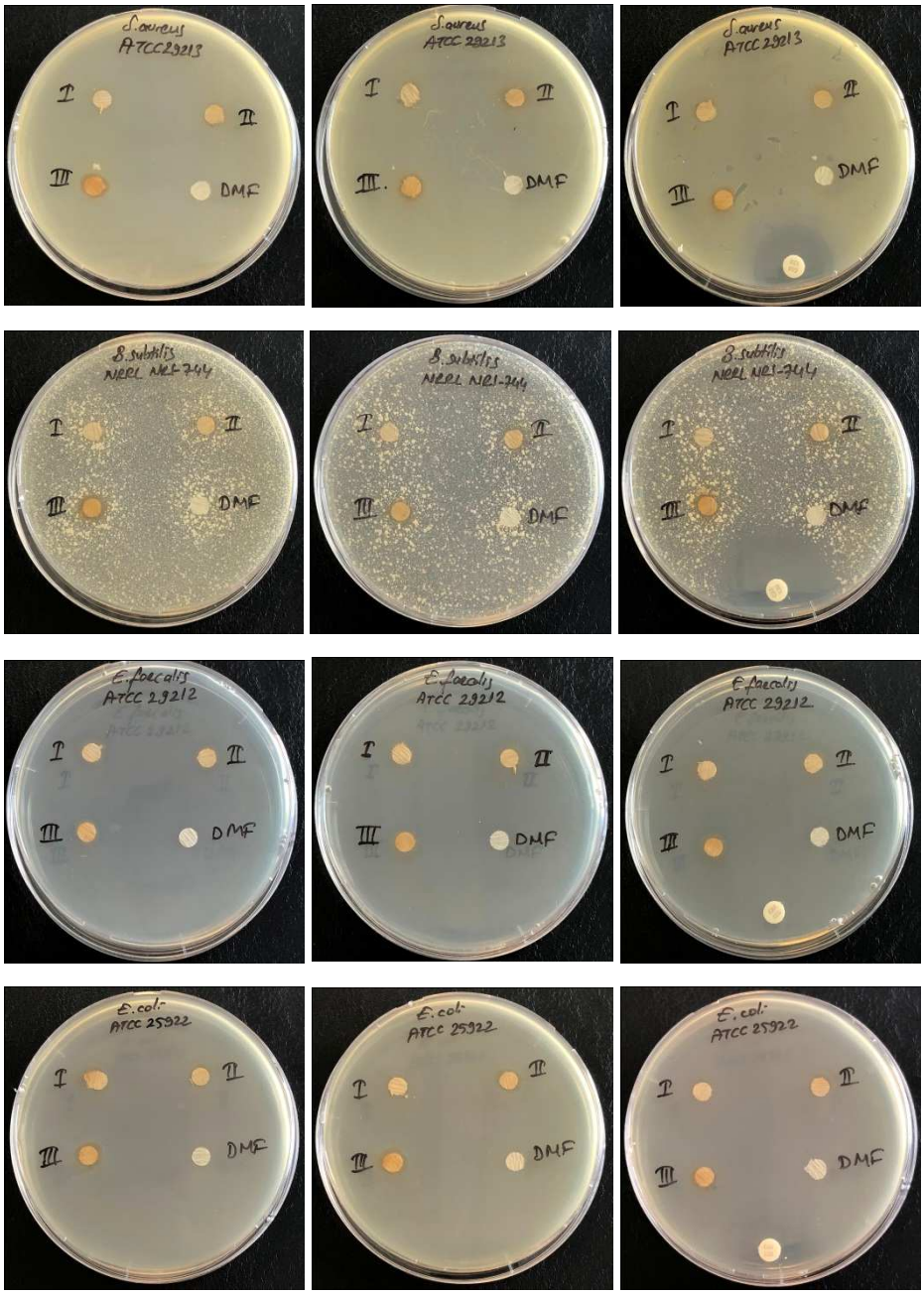

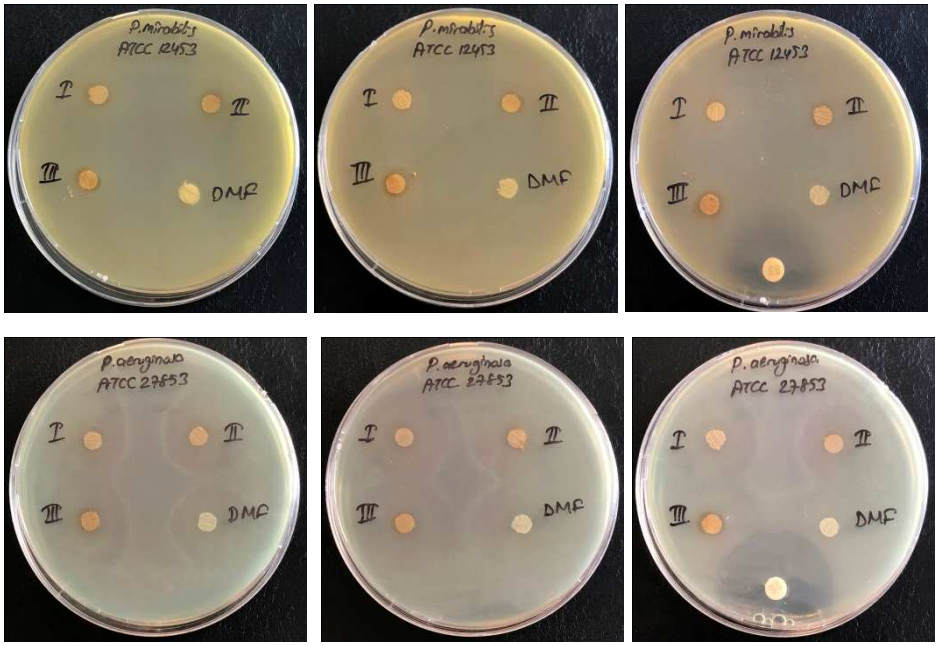

Figure 8. Antibacterial activity of fabricated nanofibers containing 3 different concentrations of Fe_3O_4@Cs@Ag magnetic nanofibers (5%, 7.5% and 10%) against six different bacteria. DMF and Fe_3O_4@Cs@Ag solutions used in the preperation of nanofibers are also tested for antibacterial activity as controls.

In order to explain the antibacterial activity of PVP nanofibers containing Fe_3O_4@Cs@Ag nanoparticles, one should take into consideration that there are four components in the structure; PVP, Fe_3O_4, Cs and Ag. So the total antibacterial efficiency will be caused by the synergistic effect of each components having antibacterial effect. It is known that PV itself does not have antibacterial effect. ***Abd El-Mohdy and Ghanem (2009)*** stated that no antibacterial activities of PVA/PVP hydrogels of various compositions were detected [60]. On the other hand, ***Prabhu et al. (2015)*** observed the antibacterial effect of Fe_3O_4 against both gram-positive and gram-negative bacteria. The presence of reactive oxygen species (ROS) generated by different nanoparticles induced the bactericidal activity. It was indicated that the antibacterial activity of Fe_3O_4 could be caused by the chemical interaction of hydrogen peroxide with membrane proteins or between the chemical produced in the presence of Fe_3O_4 nanoparticles and the outer

bilayer of bacteria. Furthermore, it was stated that the electromagnetic attraction between metal nanoparticles carrying positive charge and microbes with negative charge created the possible mechanism of action. Microbes get oxidized and died instantly as a result of the attraction between the metal nanoparticles and the microbes [61].

Another component in the structure is Ag whose antibacterial effect was widely investigated in literature and well explained. In literature there are different explanations related to the action mechanism of metal ions. One of the proposed mechanisms expresses that the metal ions can catalyze the production of oxygen radicals which are able to oxidize the molecular structure of bacteria. Such a mechanism does not need any direct contact between the anti-bacterial agent and bacteria, because the active oxygen produced diffuses from the fiber to the surrounding environment. Therefore, this mechanism could be valid in this study as Ag atoms are in bonded form in the produced nanofiber structure. Metal atoms in the nanocomposite structure catalyze the transformation of water coming from humidity present in the medium firstly to hydrogen peroxide by the action of atmospheric oxygen and then to active oxygen, as shown in the reaction given below [62, 63].

$$H_2O + 1/2\ O_2 \xrightarrow{\text{Metal ion}} H_2O_2 \Longrightarrow H_2O + (O)$$

An interesting finding published in literature is that the antibacterial effectiveness of silver is stronger when it is bound with Fe_3O_4 [64].

On the other hand, different mechanisms were mentioned in the literature regarding the antibacterial action of chitosan. The possible mechanism amongst, which would be valid in this study, is that it adsorbs and precipitates electronegatively charged substances in the cell and causes cell death by deforming the physiological activities of the cell due to its polycationic nature [65].

Results given in Table 3 and Figure 8 present that antibacterial effect of Fe_3O_4@Cs@Ag nanofibers were good against *S. aureus*, *E. faecalis*, *E. coli*, *P. mirabilis* and *P. aeruginosa*, on the other hand it showed lower antibacterial effect against *B. subtilis* than others. The highest antibacterial activities were obtained against *E. faecalis* and *E. coli* among all microorganisms. The highest concentration (III) of Fe_3O_4@Cs@Ag had good antibacterial effect on all microorganisms except *B. subtilis*. When the results were evaluated, the increasing of Fe_3O_4@Cs@Ag nanocomposite concentration was found to be effective in antibacterial activity.

4. Conclusion

Fe_3O_4@Cs nanocomposite was synthesized via a simple reflux method while the synthesis of Fe_3O_4@Cs@Ag magnetic nanocomposites was carried out in an ultrasonic bath. Obtained nanocomposites were used to produce Fe_3O_4@Cs@Ag containing magnetic nanofibers, which were produced from solution via a single capillary electrospinning device. The characterization of produced nanofibers were carried out via FT-IR, XRD, SEM-EDX, TGA, and VSM. The antibacterial effect of the nanofibers against gram negative and gram positive bacteria was also investigated.

FT-IR spectogams confirmed the successful production of magnetic nanofibers, that was also supported by the results obtained from EDX and XRD. EDX spectras indicated that produced nanofibers contained both Fe and Ag, and their amount increased with the increase in Fe_3O_4@Cs@Ag concentration in the electrospinning solution. The existence of both Fe_3O_4 ((220), (311)) (JCPDSNo.75-0033)) and Ag (111) (JCPDSNo.87-0720) was confirmed in XRD patterns of MNFs containing 7.5% and 10% of Fe_3O_4@Cs@Ag. The uniformity of produced magnetic nanofibers were seen in the images obtained from SEM. The results obtained from

VSM analysis indicated that produced nanofibers showed soft superparamagnetic behavior at room temperature. Furthermore, antibacterial test results of produced Fe_3O_4@Cs@Ag MNFs showed that the concentration of Fe_3O_4@Cs@Ag in nanofibres was an important parameter, and Fe_3O_4@Cs@Ag MNFs can be good candidates to be used in applications where magnetic and antibacterial properties are required. Therefore, it is could be possible to use Fe_3O_4@Cs@Ag nanocomposites for electromagnetic shielding purposes. However, for obtaining electromagnetic shielding effect, the most important parameter is the weight and thickness of the material. Therefore, electromagnetic shielding property was not tested since very thin layers of nanowebs were produced in this study. Nevertheless, using this compound in composite structures having both electromagnetic shielding and antibacterial effects is in our further study plans.

Acknowledgments

This work was supported in part by Scientific Research Unit of Namık Kemal University within NKUBAP.06.GA.19.195 coded project. Magnetic Characterization at Virginia Commonwealth University was partially supported by National Science Foundation, Award Number: 1726617.

References

1. T. Amna , M.S. Hassan, H. Van Ba, Electrospun Fe_3O_4/TiO_2 hybrid nanofibers and their *in vitro* biocompatibility: Prospective matrix for satellite cell adhesion and cultivation, Mater. Sci. & Eng. C 2 (2013) 707-713.
2. N. Bhardwaj, S.C. Kundu, Electrospinning: a fascinating fiber fabricationtechnique, Biotechnol. Adv. 28 (2010) 325–347.
3. A. Baji, Y.W. Mai, S.C. Wong, M. Abtahi, P. Chen, Electrospinning of polymernanofibers: effects on oriented morphology, structures and tensile properties, Compos. Sci. & Technol. 70 (2010) 703–718.
4. J. Aldana, N. Lavelle, Y. Wang, X. Peng, Size-dependent dissociation pH ofthiolate ligands from cadmium chalcogenide nanocrystals, J. Am. Chem. Soc.,127 (2005) 2496–2504.

5. S.K. Poznyak, N.P. Osipovich, A. Shavel, D.V. Talapin, M.Y. Gao, A. Eychmuller,et al., Size-dependent electrochemical behavior of thiol-capped CdTenanocrystals in aqueous solution, J. Phys. Chem. B 109 (2005) 1094–1100.

6. S. Thenmozhi, N. Dharmaraj, K. Kadirvelu, H.Y. Kim, Electrospun nanofibers: New generation materials for advanced applications, Mater. Sci. & Eng. B 217 (2017) 36–48.

7. P. Chen, H. Li, S. Song, X. Weng, D. He, Y. Zhao, Adsorption of dodecylamine hydro-chloride on graphene oxide in water, Results Phys (2017) 2281–2288.

8. Á. de J. Ruíz-Baltazar, S.Y. Reyes-López, R. Pérez, Magnetic structures synthesized by controlled oxidative etching: structural characterization and magnetic behavior, Results Phys (2017) 1828–1832.

9. A.O. Baskakov, A.Y. Soloveva, Y.V. Ioni, S.S. Starchikov, I.S. Lyubutin, I.I. Khodos, A.S: Avilov, S.P. Gubin, Magnetic and interface properties of the core-shell Fe_3O_4/Au na-nocomposites, Appl Surf Sci (2017) 638–644.

10. E. Mohammadiyan, H. Ghafuri, A. Kakanejadifard, Synthesis and characterization of a magnetic Fe_3O_4@CeO_2nanocomposite decorated with Ag nanoparticle and investigation of synergistic effects of Ag on photocatalytic activity, Optik (Stuttg) (2018) 39–48.

11. H. Noureddini, X. Gao, R.S. Philkana, Bioresour. Technol. 96 (2005) 769–777.

12. A.K. Gupta, M. Gupta, Biomaterials 26 (2005) 3995–4021

13. J.H. Lee, Y.M. Huh, Y.W. Jun, J.W. Seo, J.T. Jang, H.T. Song, S. Kim, E.J. Cho, H.G. Yoon, J.S. Suh, J. Cheon, Artificially engineered magnetic nanoparticles for ultrasensitive molecular imaging, Nat Med 13 (2007) 95–99.

14. H.E. Ghandoor, H.M. Zidan, M.H. Khalil, M.I.M. Ismail, Synthesis and some physical properties of magnetite (Fe_3O_4) nanoparticles, Int J Electrochem Sci 7 (2012) 5734–5745.

15. S. Bao, K. Li, P. Ning, J. Peng, X. Jin, L.H. Tang,. Synthesis of amino-functionalization magnetic multi-metal organic framework (Fe_3O_4/MIL-101($Al_{0.9}Fe_{0.1}$)/NH_2) for efficient removal of methyl orange from aqueous solution. J Taiwan Inst Chem E 87 (2018) 64–72.

16. K. Kamari, A. Taheri, Preparation and evaluation of magnetic core-shell mesoporous molecularly imprinted polymers for selective adsorption of amitriptyline in biological samples, Taiwan Inst Chem E 86 (2018) 230–239.

17. A.K. Singh, O.N. Srivastava, K. Singh, Shape and Size-Dependent Magnetic Properties of Fe3O4 Nanoparticles Synthesized Using Piperidine, Nanoscale Research Letters 12 (2017) 298.

18. S. Singamaneni, V.N. Bliznyuk, C. Binek, E.Y. Tsymbal, Magnetic nanoparticles: recent advances in synthesis, self-assembly and applications, J. Mater. Chem. 21 (2011) 16819-16845.

19. T. Xie, L. Xu, C. Liu, Synthesis and properties of composite magnetic material $SrCo_xFe_{12-x}O_{19}$(x= 0-0.3), Powder Technol. 232 (2012) 87-92.

20. T. An, J. Chen, X. Nie, G. Li, H. Zhang, X. Liu, H. Zhao, Synthesis of Carbon Nanotube–Anatase TiO2 Sub-micrometer-sized Sphere Composite Photocatalyst for Synergistic Degradation of Gaseous Styrene. ACS Appl. Mater. & Interfaces 4 (2012) 5988-5996.

21. H. Teymourian, A. Salimi, S. Khezrian, Fe_3O_4 magnetic nanoparticles/reduced graphene oxide nanosheets as a novel electrochemical and bioeletrochemical sensing platform, Biosens. Bioelectron 49 (2013) 1-8.

22. B. Zhang, Y. Du, P. Zhang, H. Zhao, L. Kang, X. Han, P. Xu, Microwave absorption enhancement of Fe_3O_4/polyaniline core/shell hybrid microspheres with controlled shell thickness, J. Appl. Sci. 130 (2013) 1909–1916.

23. M. Rashad, I. Ibrahim, Structural, microstructure and magnetic properties of strontium hexaferrite particles synthesised by modified coprecipitation method, Mater. Technol. 27 (2012) 308-314.

24. N.A. Frey, S. Peng, K. Cheng, S. Sun, Magnetic nanoparticles: synthesis, functionalization, and applications in bioimaging and magnetic energy storage, Chem. Society Rev. 38 (2009) 2532-2542.

25. Md. Amir, S. Güner, A. Yıldız, A. Baykal, Magneto-optical and catalytic properties of Fe_3O_4@HA@Ag magnetic nanocomposite, J. of Magnetism & Magn. Mater. 421 (2017) 462-471.

26. T.K. Indira, P.K. Lakshmi, Magnetic Nanoparticles: A Review, Int. J. Pharm. Sci. & Nanotechnol. 3 (2010) 1035-1042.

27. S. Suzuki, Biological effects of chitin, chitosan, and their oligosaccharides, Biotherapy. 14 (2000) 965–971.

28. M.N.V. Kumar, A review of chitin and chitosan applications, Reactive Funct Polym. 46 (2000) 1–27.

29. R.A. Muzzarelli, Chitin, Pergamon Press (1977) Oxford, UK,

30. R.A. Muzzarelli, C. Muzzarelli, Chitosan chemistry: Relevance to the biomedical sciences. Adv Polym Sci. 186 (2005) 151–209.

31. R.N. Tharanathan, F.S. Kittur, Chitin – the undisputed biomolecule of great potential, Crit Rev Food Sci Nutr. 43 (2003) 61–87.

32. Y. Shigemasa, S. Minami, Applications of chitin and chitosan for biomaterials, Biotechnol Genet Eng Rev. 13 (1995) 383–420.

33. I. Aranaz, M. Mengibar, R. Harris, I. Paňos, B. Miralles, N. Acosta, G. Galed, A. Heras, Functional characterization of chitin and chitosan, Curr Chem Biol. 3 (2009) 203–230.

34. S.S. Koide, Chitin-Chitosan: Properties, benefits and risks, Nutr Res. 18 (1998) 1091–1101.

35. M.V. Kumar, S.M. Hudson, Chitosan. In: Wnek GE, Bowlin GL, editors. Encyclopedia of Biomaterials and Biomedical Engineering. New York: Marcel Dekker (2004) 310–323.

36. M. Kong, X.G. Chen, K. Wing, H.J. Park, Antimicrobial properties of chitosan and mode of action: a state of the art review, Int J Food Microbiol. 144 (2010) 51-63.

37. J.C. Fernandes, F.K. Tavaria, J.C. Soares, O.S. Ramos, M. JoaoMonteiro, M.E. Pintado, F. Xavier Malcata, Antimicrobial effects of chitosans and chitooligosaccharides, upon Staphylococcus aureus and Escherichia coli, in food model systems, Food Microbiology 25 (2008) 922-928.

38. Y. Wang, P. Zhou, J. Yu, X. Pan, P. Wang, W. Lan, S. Tao, Antimicrobial effect of chitooligosaccharides produced by chitosanase from Pseudomonas CUY8, Asia Pacific Journal of Clinical Nutrition, 16 (2007) 174-177.

39. E.J. Yang, J.G. Kim, J.Y. Kim, S. Kim, N. Lee, C.K. Hyun, Anti-inflammatory effect of chitosan oligosaccharides in RAW 264.7 cells, Central European Journal of Biology 5 (2010) 95-102.

40. H. Quan, F. Zhu, X. Han, Z. Xu, Y. Zhao, Z. Miao, Mechanism of anti-angiogenic activities of chitooligosaccharides may be through inhibiting heparanase activity Medical Hypotheses 73 (2009) 205-206.

41. R. Pangestuti, S.K. Kim, Neuroprotective properties of chitosan and its derivatives Marine Drugs 8 (2010) 2117-2128.

42. R. Abdulla, M.H. Nişancı, A.H. Yüzer, Statistical Analysis of Electromagnetic Shielding Effectiveness of Metal Fiber Blended Fabrics, Süleyman Demirel University J. Natural & Appl. Sci. 21 (2017) 711-717.

43. N.O.S. Yurudu, A.K. Erdem, N.Ş. Yurudu, The Evaluation of Antibacterial Activity of Fabrics Impregnated with Dimethyltetradecyl (3-(Trimethoxysilyl) Propyl) Ammonium Chloride, IUFS J Biol, 67 (2008) 115-122.

44. M. Polichetti, M. Modestino, A. Galluzzi, S. Pace, M. Iuliano, P. Ciambelli, M. Sarno, Influence of citric acid and oleic acid coating on the dc magnetic properties of Fe_3O_4 magnetic nanoparticles, Mater. Today Proc. (2020) 21-24.

45. V.K. Sharma, R.A. Yngard, Y. Lin, Silver nanoparticles: Green synthesis and their antimicrobial activities, Adv. in Colloid & Interface Sci. 145 (2009) 83-96.

46. C.N. Lok, C.M. Ho, R. Chen, Q.Y. He, W.Y. Yu, H. Sun, P.K. Tam, J.F. Chiu, C.M. Chen, Proteomic analysis of the mode of antibacterial action of silver nanoparticles, J. Proteome. Res. 5 (2006) 916-924.

47. K.H. Cho, J.E. Park, T. Osaka, S.G. Park, The study of antimicrobial activity and preservative effects of nanosilver ingredient, Electrochimica Acta 51 (2005) 956-960.

48. S. Silver, Bacterial silver resistance: molecular biology and uses and misuses of silver compounds, FEMS Microbiol. Rev. 27 (2003) 341-353.

49. A. Yildiz, R. Atav, M. Oztas, A.Ö. Ağirgan, D. Gülen, M. Aydin, M. Yeşilyurt, A.D. Kaya, Synthesis of Silver Mono- and Di-Carboxylates and Investigation of their Usage Possibility in Textiles as an Antibacterial Agent, Fibres & Textiles in Eastern Europe 23 (2015) 120-125.

50. C. Demir, Fe_3O_4@HA@Ag Sentezi, Yapısının İncelenmesi ve Tekstilde Kullanımı, Tekirdağ Namık Kemal Üniversitesi Fen Bilimleri Enstitüsü Tekstil Mühendisliği Anabilim Dalı, Master Thesis, (2018) Tekirdağ.

51. R. Atav, A.O. Agirgan, D.V. Bayramol, A.Yildiz, Inclusion complexes of β-cyclodextrine with Fe3O4@HA@Ag Part I: Preparation and characterization, Industria Textila 70 (2019) 255-258.

52. C. Cao, L. Xiao, C. Chen, X. Shi, Q. Cao, L. Gao, In situ preparation of magnetic Fe3O4/chitosan nanoparticles via a novel reduction–precipitation method and their application in adsorption of reactive azo dye, Powder Technology 260 (2014) 90–97.

53. X.N. Pham, T.P. Nguyen, T.N. Pham, T.T.N. Tran, T.V.T. Tran, Synthesis and characterization of chitosan-coated magnetite nanoparticles and their application in curcumin drug delivery, Adv. Nat. Sci.: Nanosci. Nanotechnol. 7 (2016) 045010.

54. Md. Amir, U. Kurtan, A. Baykal, Rapid color degradation of organic dyes by Fe_3O_4@His@Ag recyclable magnetic nanocatalyst, J. Industrial & Eng. Chem. 27 (2015) 347-353.

55. U. Kurtan, E. Onuş, Md. Amir, A. Baykal, Fe_3O_4@Hpipe-4@Cu Nanocatalyst for Hydrogenation of Nitro-Aromatics and Azo Dyes, J. Inorg. & Organomet. Polymers & Mater. 25 (2015) 1120–1128.

56. Y. Wei, B. Han, X. Hu, Y. Lin, X. Wang, X. Deng, Synthesis of Fe_3O_4 nanoparticles and their magnetic properties, in Procedia Engineering, 27 (2012) 632–637.

57. M. Anbarasu, M. Anandan, E. Chinnasamy, V. Gopinath, K. Balamurugan, Synthesis and characterization of polyethylene glycol (PEG) coated Fe_3O_4 nanoparticles by chemical co-precipitation method for biomedical applications, Spectrochim. Acta. A. Mol. Biomol. Spectrosc. 135 (2015) 536–539.

58. C. Nayek, K. Manna, G. Bhattacharjee, P. Murugavel, I. Obaidat, Investigating Size- and Temperature-Dependent Coercivity and Saturation Magnetization in PEG Coated Fe_3O_4 Nanoparticles, Magnetochemistry 3 (2017) 19.

59. R.L. Hadimani, Y. Melikhov, M. Han, D.C. Jiles, Magnetocrystalline Anisotropy in Single Crystal $Gd_5Si_{2.7}Ge_{1.3}$, IEEE Trans. Magn. 48 (2012) 3989-3991.

60. H.L. Abd El-Mohdy, S. Ghanem, Biodegradability, antimicrobial activity and properties of PVA/PVP hydrogels prepared by γ-irradiation. J Polym Res. 16 (2009) 1622.

61. Y.T. Prabhu, K. Venkateswara Rao, B. Siva Kumari, V.S. Sai Kumar, T. Pavani, Synthesis of Fe3O4 nanoparticles and its antibacterial application. Int Nano Lett. 5 (2015) 85-92.

62. R. Dastjerdi, M. Montazer, A review on the application of inorganic nano-structured materials in the modification of textiles: Focus on anti-microbial properties. Colloids and Surfaces B: Biointerfaces 79 (2010) 5-18.

63. A. Yildiz, R. Atav, M. Oztas, A.O. Agirgan, D. Gulen, M. Aydin, M. Yesilyurt, A.D. Kaya, Synthesis of Silver Mono- and Di-Carboxylates and Investigation of their Usage Possibility in Textiles as an Antibacterial Agent, Fibres&Textiles in Eastern Europe 23 (2015) 120-125.

64. A. Pachla, Z. Lendzion-Bieluń, D. Moszyński, A. Markowska-Szczupak, U. Narkiewicz, R.J. Wróbel, N. Guskos , G. Żołnierkiewicz, Synthesis and antibacterial properties of Fe_3O_4-Ag nanostructures, Polish Journal of Chemical Technology, 18 (2016) 110-116.

65. A. Demir, T. Öktem, N. Seventekin, Kitosanın Tekstil Sanayiinde Antimikrobiyal Madde Olarak Kullanımının Araştırılması, Tekstil ve Konfeksiyon 2 (2008) 94-102.

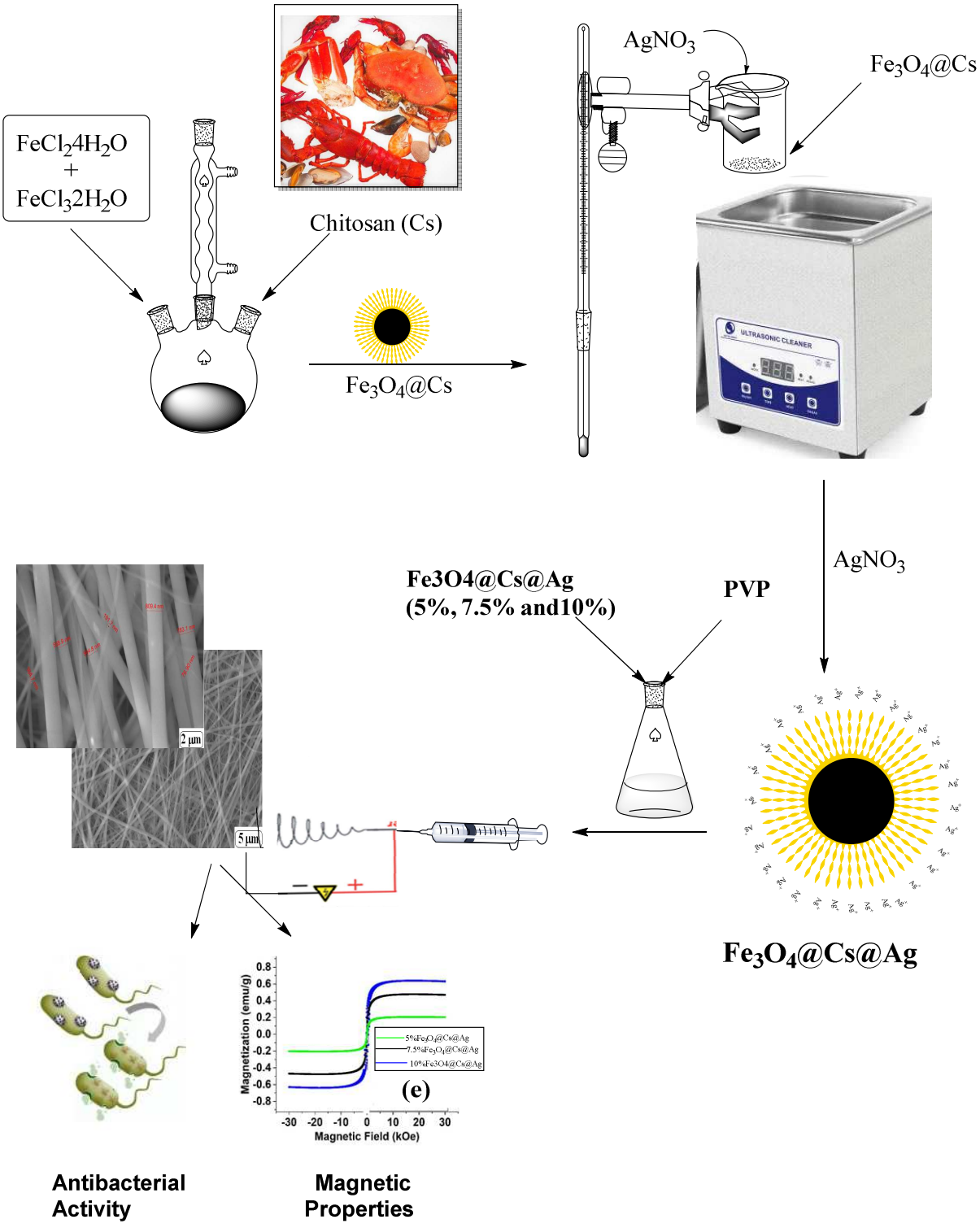
FeCl2 4H2O
+
FeCl3 2H2O
Chitosan (Cs)
Fe3O4@Cs
AgNO3
Fe3O4@Cs
ULTRASONIC CLEANER
AgNO3
Fe3O4@Cs@Ag
(5%, 7.5% and10%)
PVP
Fe3O4@Cs@Ag
2 µm
5 µm
Magnetization (emu/g)
Magnetic Field (kOe)
5%Fe3O4@Cs@Ag
7.5%Fe3O4@Cs@Ag
10%Fe3O4@Cs@Ag
(e)
Antibacterial Activity
Magnetic Properties